Essential Readings in Light Metals: Cast Shop for Aluminum Production.
Edited by John F. Grandfield and Dmitry G. Eskin.

GAS FLUXING OF MOLTEN ALUMINUM
Part 1: Hydrogen Removal

Geoffrey K. Sigworth

GKS Engineering Services
116 Derby Street, Johnstown, PA 15905
e-mail: gkseng@twd.net

Abstract

The aluminum industry is under continual pressure to improve metal quality, while at the same time reduce costs. The only way to do this is through continual process optimization. Although the gas fluxing of aluminum is a reasonably mature technology, there is still room for improvement. A detailed review and theoretical analysis is given for chemical and kinetic factors which control the metal quality after gas fluxing, and suggestions are made for ways to improve the process. Particular emphasis is placed on hydrogen removal and minimization of chlorine use. Considerations related to inclusion removal are also discussed briefly.

Introduction

In order to understand any chemical process, we must consider two fundamental aspects. The first is the rate at which mass transport and important chemical reactions occur. The second is the thermodynamic equilibrium state associated with the process, which becomes limiting when the kinetics of the process is rapid.

Because high temperatures are present in the refining of molten metals, and because the energy available for chemical reactions, in the form of thermal fluctuations, is proportional to the thermodynamic temperature, chemical reactions usually proceed to equilibrium rapidly. In practice this means that a molten metal process will usually be controlled by mass transport of reacting species (by diffusion and convection) or by the thermodynamic equilibrium state. Fortunately, gas fluxing of aluminum is not an exception to this rule.

The important thermodynamic and kinetic aspects of gas fluxing are considered below.

Hydrogen Solubility in Pure Aluminum

A survey of the literature shows that three reviews have been published on the solubility of hydrogen in aluminum melts. The first is the paper by Sigworth and Engh [1], published in 1982. The second is the 1989 study of Lin and Hoch [2]. Unfortunately, the data in this paper is presented in a format which is not convenient to use. The most recent, and therefore most complete, is the 1995 review by Anyalebechi [3].

The solubility of hydrogen in pure aluminum is usually represented by the symbol S, and gives the amount of gas[1] present in liquid metal at equilibrium with pure hydrogen at one atmosphere pressure. The solubility is usually given in units of cubic centimeters of gas (at standard temperature and pressure) per 100 grams of metal, and this is the concentration employed herein, unless specified otherwise.[2]

A number of equations have been given for the gas solubility. The thermodynamic temperature, T, in degrees Kelvin, is used in Table I. The equations proposed and the value of S at 1000 °K (727 °C or 1340 °F) are shown. With the exception of the value proposed in reference [5], there is little difference between the published values. Reference 4 is an experimental study undertaken by Talbot and Anyalebechi to establish the value of hydrogen solubility, which was put into question by the study of Eichenauer and co-workers [6]. Eichenauer used a different experimental technique, which appears to be unreliable. An excellent discussion of the probable errors is given in [4]. Unfortunately, San-Martin and Manchester used Eichenauer's results in their assessment of the phase diagram for the Al-H system. Not only is the solubility given in this review much too high, but the equation employed is not justified from a thermodynamic point of view.

Table I. Hydrogen Solubility in Pure Aluminum

equation	S at 1000 K	source
$\log S = -2750/T + 2.767$	1.040	Telegas
$\log S = -2760/T + 2.796$	1.086	Alscan
$\log S = -2550/T + 2.620$	1.175	[1]
$\log S = -2692/T + 2.726$	1.081	[3]
$\log S = -2700/T + 2.720$	1.047	[4]
$S = 6.517 - 0.021T + 0.18\times10^{-5}T^2$	3.533	[5]

The equation given in reference [3] is probably the most accurate and reliable of the equations given above, and has been underlined. It gives a value for gas solubility almost exactly equal to the value used in the Alscan unit, and it is different from the value used in Telegas by less than 4%. This equation was obtained by a regression analysis of the data given in the nine most reliable experimental studies.

The solubility, S, represents the equilibrium constant for the reaction:

$$\tfrac{1}{2}\,H_2\ (\text{vapor}) = \underline{H}\ (\text{in Al}) \qquad (1)$$

[1] As hydrogen is the only gas which is soluble in liquid aluminum at normal casting temperatures the terms 'gas' and 'hydrogen' are used interchangeably.

[2] The following conversion factors may be used: 1 $cm^3/100g$ = 0.9 ppm = 0.9×10^{-4} wt% = 2.409×10^{-5} mole fraction

This means that the amount of gas dissolved in metal at any pressure of hydrogen is equal to $S\sqrt{P}$, where P is the pressure (in atmospheres) of hydrogen gas. This square root dependence for diatomic gases dissolved in metals was first established by the experiments of Sieverts [7,8]. In the Alscan, Telegas and DPM gas testers the pressure of hydrogen gas is measured in the melt. The amount of gas is then calculated from the pressure. The gas pressure is also measured in the TYK sensor, although indirectly, by using a high temperature solid state sensor [9].

Hydrogen Solubility in Alloys

In alloys the solubility is usually different from pure aluminum, and so a "correction factor" is applied. If the correction factor is *C*, the hydrogen content, *H*, is given by the relation:

$$H = C\,S\sqrt{P} \qquad (2)$$

We have seen above that

$$\log S = -2692/T + 2.726 \qquad (3)$$

We must now establish an equation for the correction factor, *C*.

The best way to calculate the correction factor is to use interaction coefficients. These were used first by Wagner [10] and Chipman [11], and later refined and generalized by Lupis [12] to describe activities in multi-component alloys. Interaction coefficients are based on a Taylor Series expansion of the excess Gibbs Free Energy of solution of the element under consideration. For hydrogen,

$$\log f_H = \Sigma e_H^j [\%j] + \Sigma r_H^j [\%j]^2 + \varphi \qquad (4)$$

where f_H is the activity coefficient of hydrogen in the alloy at hand, e_H^j is the first order interaction coefficient, [%j] is the weight percent of the jth alloying element (Fe, Cu, Mn, Mg etc.) dissolved in the aluminum based alloy (the solvent, Al, is element No. 1), and r_H^j is the second order interaction coefficient. The contribution of higher order terms, φ, in equation 4 can be usually neglected in most alloys. Besides generally making a small contribution, they can rarely be established by the precision of the data available to us. The correction factor, C, is equal to $1/f_H$. Or,

$$-\log C = \Sigma e_H^j [\%j] + \Sigma r_H^j [\%j]^2 \qquad (5)$$

We now look at the available data to see what values may be used for the interaction coefficients. Numerical values for interaction coefficients are given in the reviews of Sigworth and Engh [1] and Anyalebechi [3,13]. These are tabulated below for a metal temperature of 700C (1292 F). The recommended values of the interaction coefficients are underlined in the table. Values in parenthesis are considered to be estimates, as the precision of the data appears to be questionable.

Discussion of Correction Factors

Correction factors have been calculated for a number of common alloys, using the equations and interaction coefficients given above. A comparison of the "new" correction factors with older values will show that they are often significantly different. The reason for this is twofold. Firstly, the old factors were calculated from an empirical formula originally given by Hess:

$$C = 0.81[1.23-(0.0733\ \%Cu)-(0.033\%Si)+(0.0489\ \%Mg)] \qquad (6)$$

which accounts for only three elements (Cu, Si and Mg). The effect of other elements is ignored. Secondly, the form of equation 6 is not suitable from a thermodynamic point of view, whereas the formulae proposed for interaction coefficients are now well established.

The author has written a computer program which calculates correction factors for most common alloys, and would be pleased to provide this on request.

Table II. Interaction Coefficients for Hydrogen in Aluminum Melts

Coefficient	Value, Ref. [1]	Value, Ref [3,13]
e_H^{Ce}	(-0.08)	---
e_H^{Cu}	0.03	0.0334*
r_H^{Cu}	-0.0004	-0.00065*
e_H^{Cr}	(0)	---
e_H^{Fe}	(0)	0.0659*
e_H^{Li}	---	-0.25
e_H^{Mg}	(-0.01)	-0.066
e_H^{Mn}	(0.06)	---
e_H^{Ni}	(0.04)	---
e_H^{Si}	0.03	0.0193*
r_H^{Si}	-0.0008	-0.00045*
e_H^{Sn}	0.004	---
e_H^{Th}	-0.006	---
e_H^{Ti}	(-0.1)	-0.0205*
e_H^{Zn}	---	0.0163*
e_H^{Zr}	---	-0.808

Notes:
*These coefficients vary with temperature. For temperatures other than 700 C, consult ref. [3,13].

Kinetics of Hydrogen Removal

The kinetics of hydrogen removal was studied in detail by Sigworth and Engh [1,14]. A schematic view of the degassing process is given below in Figure 1. This Figure shows a cross sectional view of a rotary impeller degasser. Small bubbles of an insoluble gas (usually argon or nitrogen) are introduced near the bottom of the melt. As they float upwards towards the surface,

hydrogen dissolved in the metal diffuses into the bubbles. The hydrogen gas is carried up to the surface with the inert gas, and removed when the bubbles leave the melt.

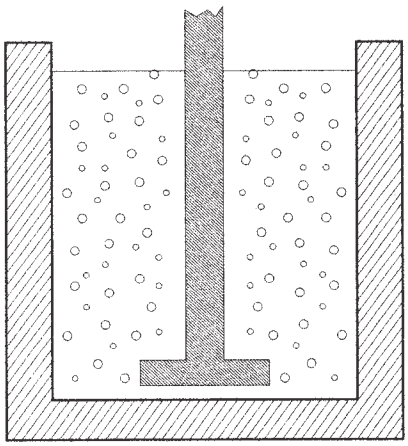

Figure 1. Schematic View of Degassing Process

The degassing process can be considered in one of two ways. One is to examine what happens to a single bubble as it floats up towards the surface. The usual procedure is to follow the chemical engineering approach, and use a semi-empirical mass transfer coefficient, k, to characterize the transport of gas to the bubble. Botor [15] conducted extremely detailed experiments of single bubbles rising through aluminum melts in the laboratory, and gave values for the mass transfer coefficient as a function of temperature, bubble diameter and gas composition.[3] These results are summarized in [1], and for bubbles larger than about one millimeter can be represented [16] by the equation:

$$k = 2\sqrt{\frac{DU}{\pi d}} \tag{7}$$

where D is the diffusion coefficient of hydrogen, U is the steady state rise velocity of the bubble, and d is the diameter of the bubble.[4] The steady state rise velocity of the bubble is:

$$U = \sqrt{\frac{gd}{2}} \tag{8}$$

where g is the gravitational constant. This means that the mass transfer coefficient is equal to:

$$k = 2\sqrt{\frac{D}{\pi}} \cdot \left(\frac{g}{2d}\right)^{1/4} \tag{9}$$

[3] The presence of 10% chlorine in the purge gas increases the rate of hydrogen diffusion to the bubble by a factor of two [15]. As we shall see below, however, in most industrial systems this has no beneficial effect on the overall rate of gas removal. The chlorine does affect inclusion removal, however.

[4] This equation also applies to other elements reacting with the bubble, like sodium. In this case the diffusion coefficient of sodium would be used.

The other way to consider the degassing process is to model a small volume of the melt, as shown in Figure 2. The procedure is to construct a mass balance along the height ΔH. The contact area of the bubbles in this volume is ΔA. Because of the stirring associated with the rotating impeller, and the ascent of the bubbles, we assume that the metal composition is everywhere the same, and equal to the exit composition, C_e. The composition of the gas changes, however, as it rises through the melt, and results in a change in pressure of the reacting species, ΔP. The amount of metal flowing through the unit is $\dot{M}$. The gas flow rate is $\dot{G}$.

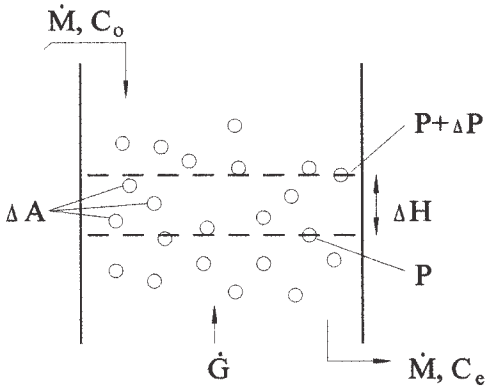

Figure 2. Control Volume for Gas Fluxing

The control volume is used to construct a differential equation, which is then integrated from the bottom to the top of the melt. The mathematics is given in [1], and is extremely complex, principally because of the factor of one-half in equations 1 and 2. What is important to note here is that a degassing process can be described by a "dimensionless hydrogen concentration", given (at atmospheric pressure) by the formula:

$$\psi / \underline{H} = \frac{k\rho A \cdot C^2 S^2}{B' \cdot \dot{G}} \cdot \frac{1}{\underline{H}_e} \tag{10}$$

where ρ is the density of aluminum (c. 2700 kg/m^3), A is the area of bubbles (m^2) in the reactor at any time, and $\underline{H}_e$ is the exit gas content. B' is a constant whose value depends on the units used for G. When the gas flow is given in liters/minute, B' is numerically equal to 3.32.

Figure 3 shows the approach to equilibrium for the degassing process, as a function of the dimensionless hydrogen concentration. When $\psi / \underline{H}$ is greater than about 1.5, the gas bubbles exiting the bath are nearly saturated with hydrogen.

The practical implications are best seen by an example calculation given in [14], where the degassing efficiency for a 250 kg (550 lb.) crucible furnace is shown as a function of bubble diameter for two different gas contents. The results are plotted in Figure 4. Note that we operate at a degassing efficiency close to 100 % when the bubble size is less than about 5 millimeters. The reason for this may be seen by considering equation 10. The surface area of the bubbles in the melt, A, increases sharply as the bubble size decreases.

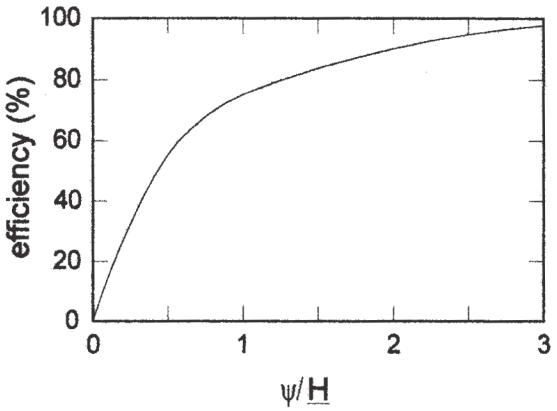

Figure 3. Degassing Efficiency vs. $\psi / \underline{H}$

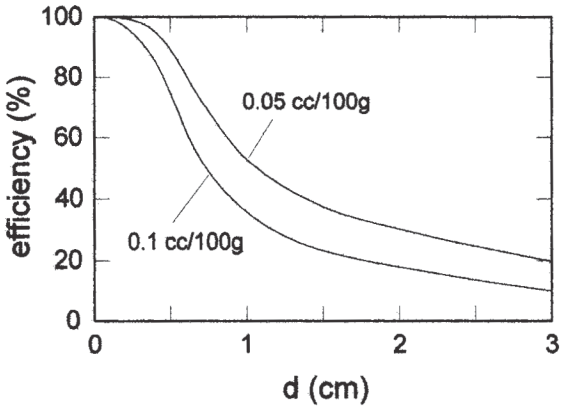

Figure 4. Degassing Efficiency vs. Bubble Size

For example, if one halves the bubble size, the surface area of an individual bubble increases by a factor of four times. But the rise velocity of the bubble decreases also, according to equation 8. This means that individual bubbles stay in the melt longer, which further increases the bubble surface area in the melt. The two effects are additive, and so the dimensionless hydrogen concentration, and the process efficiency, increase sharply as we produce smaller bubbles.

The practical implications of this analysis are obvious. In most industrial degassing processes (SNIF, ALPUR, etc.) we produce bubbles that are on the order of 5 mm in diameter or less [16]. This means that, in most cases, we should be operating close to thermodynamic equilibrium.

Although it is given elsewhere [1,14] it will be instructive to derive an equation for the degassing process shown schematically in Figure 2. A mass balance for this in-line reactor is given by:

$$10\dot{M}\left(\underline{H}_o - \underline{H}_e\right) = 1000\dot{G}\frac{P}{P_{inert}} \tag{11}$$

where

$\dot{M}$ is the metal flow in kg/min

$\underline{H}_o$ and $\underline{H}_e$ are the original and exit gas contents of the metal, in cc/100g

$1000\dot{G}$ is the inert gas flow in cc/min, when $\dot{G}$ is in l/min, and

P and P_{inert} are in atmospheres

As noted above, the purge gas will be almost saturated with hydrogen, and at thermodynamic equilibrium. So,

$$\underline{H}_e \cong CS\sqrt{P} \tag{12}$$

and

$$10\dot{M}(\underline{H}_o - \underline{H}_e) = 1000\frac{\dot{G}}{P_{inert}}\left(\frac{C\underline{H}_e}{S}\right)^2$$

or

$$\underline{H}_e^2 = -\beta\underline{H}_e + \beta\underline{H}_i \tag{13}$$

where

$$\beta = \frac{\dot{M}P_{inert}C^2S^2}{100\cdot\dot{G}} \tag{14}$$

The term β has the same units as the gas content (cc/100g) and describes the ratio of the two flows in the process; metal and gas; and their relative capacity to carry the hydrogen out of the system. Equation 13 is a simple quadratic equation, having two roots. The positive root gives the gas content in the metal as it exits the treatment box:

$$\underline{H}_e = -\beta/2 + 1/2\sqrt{\beta^2 + 4\beta\underline{H}_i} \tag{15}$$

When the term $\dot{M}$ in Figure 2 is zero, we have a batch gas fluxing process. In this case the hydrogen content in the metal decreases with time [1, 13], according to the equation:

$$\frac{1}{\underline{H}} - \frac{1}{\underline{H}_o} = \frac{t}{\tau} \tag{16}$$

where

$\underline{H}$ is the hydrogen content with time

$\underline{H}_o$ is the original hydrogen content

t is the degassing time in seconds

and where

$$\tau = 2\mathrm{MP}_{\mathrm{inert}}C^2S^2/\dot{G}B' \tag{17}$$

Equation 16 would be used for degassing in a crucible furnace or ladle.

Discussion

There are a number of interesting and useful observations that can be made from the preceding analysis.

Equations 10, 13-14 and 16-17 all contain the term S^2. The gas solubility, S, is an exponential function of temperature. This means that S^2 will double with a temperature increase of 60 °C. In the case of a batch degassing process, this means it will take twice as long to reach the desired hydrogen level.

The effect of higher temperatures on the results obtained during in-line treatments are equally dramatic. This is best seen by example. Equation 13 has been solved for a number of values of β, which are normally found in practice, and for different starting gas concentrations. Because most industrial sources report the

percent of gas removed, the results of these calculations are shown in Figure 5 using this format. Results are shown for four different values of the degassing constant, β. A 60 °C increase in temperature increases β by a factor of two. It is readily seen that a significant drop in degassing efficiency is the result.

For some reason, it has not been widely recognized that in-line degassing efficiencies depend on the original gas level. There is only one reference to this effect in the literature. (See Figure 1 of reference [19].) This is surprising, since the curves shown in Figure 5 result from the limitations on the degassing process imposed by thermodynamic equilibrium.

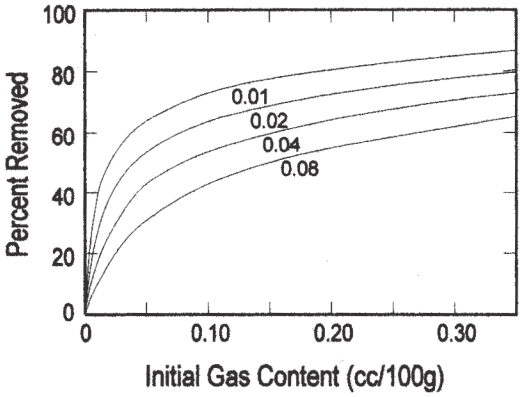

Figure 5. Calculated Degassing Efficiencies

The equations given above can also be used to predict the performance of multi stage in-line degassing systems. In this case, the calculated exit gas composition from first stage becomes the entering composition of the second stage; and so on, if there are more than two stages. The results of these calculations for a two stage system are shown below in Figure 6. The corresponding curves for a single stage unit, having the same total gas flow (and the same value of β) are also plotted for comparison. As noted before [19], the effect of staging a unit, especially at larger values of β, is not significant.

Of course, the usual reason to add an additional stage is to be able to use more gas in the fluxing process. Any rotor head will be able to deliver only a certain amount of fluxing gas. If you are operating at this maximum with a single stage unit, and need additional degassing capacity, one possible solution is to add a second stage. This will allow you to use more gas, and to move to smaller vales of β in Figure 6. Thus, the degassing efficiency (percentage of gas removed) will increase significantly.

There is another possibility, of course. It is also possible to modify the rotor design, so that it will deliver larger quantities of gas. This solution is a great deal more convenient, and less costly, than adding a second stage. For this reason, a great deal of research and development has gone into improving rotor head design.

It is beyond the scope of this paper to offer a history of rotor head design, or to present a detailed comparison of the different heads which have been used. Nor am I prepared to explain the hydrodynamic theory related to the subject. For the reader who

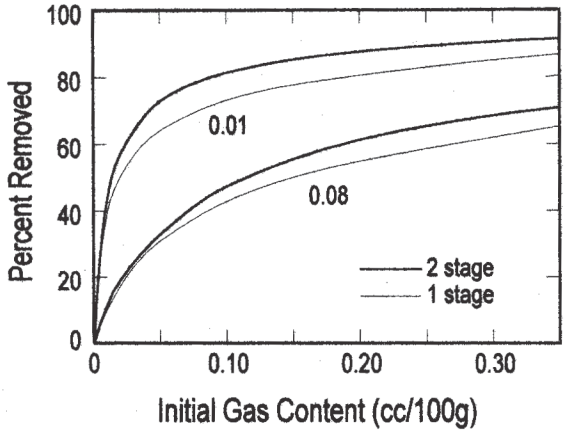

Figure 6. Degassing Efficiency of Two Stages Compared to a Single Stage

wishes to pursue this area of technology in more depth, there are several excellent publications which present a great deal of information [17-18, 20-21]. It will, however, be possible to offer some important general observations here.

Other things being equal, the degassing performance of an in-line rotor head improves when the stirring energy is increased. I learned this the hard way some years ago, when my company began to place a rotary impeller degasser (RID) designed for foundry service into the cast house. The foundry unit had been used successfully for several years in crucible furnaces and transfer ladles, with metal capacities as large as 1500 kg. In this application it was important to generate small bubbles without a great deal of stirring. This is because it was impractical to use baffle plates. So, excessive stirring caused a metal vortex, which sucked surface oxides into the melt. When this RID unit was placed into service as a replacement for in-line SNIF units, the performance was satisfactory only for low metal flow rates, less than about 125 kg/min.

We then tried a number of different rotor head designs, in order to increase the specific stirring intensity and power. The final result was a rotor head that gave equivalent or slightly better performance, than the old SNIF unit. Higher metal flow rates could be treated satisfactorily, and it was also possible to deliver higher gas flow rates.

The increase in performance observed with the new rotor head was larger than expected from the increased gas delivery. This suggests that the stirring energy produces two desirable effects: a distribution of fine bubbles, and good metal mixing. In other words, if the stirring is not adequate to fully mix the melt, some of the high gas metal entering the treatment box manages to 'slip by' without being fully treated.

The effect of stirring on bubble size and bubble distribution has been studied in great detail. The most appealing explanation, because of its simplicity, is a theory offered by our Norwegian colleagues [18]. They examined the forces acting on bubbles in a stirred melt. The surface tension force on the bubble holds it together. Viscous forces acting on the bubble, because of

turbulent shear produced by stirring, tend to break it up. Calculating and balancing the two types of forces, they were able to show the maximum bubble diameter that can exist in a stirred melt is:

$$d = \left(\frac{\sigma}{\rho}\right)^{0.6}\left(\frac{M}{E}\right)^{0.4} \qquad (18)$$

where

σ is the surface tension of the metal
ρ is the density of molten aluminum
M is the mass of metal in the chamber, and
E is the energy of stirring.

This simple relation was sufficient to allow them to calculate the bubble sizes observed in a large number of water model experiments with the HYCAST rotor. It also allowed them to deduce that the bubble size in liquid metal will be just over twice that observed in water model studies.

Of course, as the stirring intensity increases, the designer has to deal somehow with the increased amount of rotational energy placed into the metal. Otherwise a great deal of splashing, vortexing, or an air/metal emulsion are produced. Various design solutions have been placed into service, either singly or in combination:

-using baffle plates
-using rectangular boxes
-placing the rotor off center in the box
-alternating rotor direction in multi-stage units
-using 'pumping' heads, to control and direct the metal flow
-using rotor designs, having a high localized shear where gas enters the melt
-reversing rotation of the rotor assembly

The last method appears to a most promising technique, and may allow us to increase the specific stirring intensity to levels that are beyond what is considered normal today. Invented by Eckert [22], and marketed under the name REVROT, the rotation of the rotor shaft is reversed periodically at c. 5-10 second intervals. In this way the rotational momentum introduced into the melt during one cycle is largely canceled by the following reverse rotation. Very high stirring intensities are possible without the use of baffle plates, or other hydrodynamic methods, which are normally needed to avoid vortex formation.

Above we derived equations for degassing performance, which assumed the process was very close to thermodynamic equilibrium. It would be natural to ask if there is any evidence for this assertion. Fortunately there is, but it does not come from the expected sources. For some reason the major players in degassing technology (Alcoa, Alpur, HYCAST, SNIF) have not supplied suitable process data. What is required is information that is sufficiently detailed to allow us to make our own calculations. A 'predigested' data set is not adequate. For example, as noted above, information on degassing efficiency is useless unless we know the starting gas level. The alloy used and the metal temperature also have an important effect.

There is detailed process data for three different degassers: GBF [23], GILS [24] and RDU [25,26]. The published data has been analyzed by using equations 13-14. Where information has been reported for a two stage unit, it was assumed the total gas flow was divided equally between the two stages. The results of the analysis are plotted in Figure 7.

When viewing Figure 7, one must keep in mind the errors involved in the hydrogen analysis. Any errors here will show up in the degassing efficiency. A brief analysis of the errors involved suggests that the standard (1σ) deviation for measured degassing efficiency is on the order of four percentage points. This error limit is indicated by the two dotted lines in the figure.

Data for the GBF rotor follows the theoretical (thermodynamic) relationship quite closely. This degassing system uses a high speed rotor (700-900 rpm) together with a treatment box containing special baffle plates, to produce very small bubbles. Nearly 60% of the GBF data points fall within the 1σ error bands, and all but two data points fall within a ±3σ band. This data is for 11 different alloys (correction factors were calculated from equation 5) cast at rates from 42 to 612 kg/min. It therefore represents an excellent validation of the model presented here.

The GIFS and RDU data do not follow the theoretical relationship so well, and most data points fall below the theoretical. In other words, the gas removal efficiency for these units is about 5-10 percentage points below the theoretical maximum. A closer examination of the data than is presented in Figure 7, suggests that in many cases the GIFS and RDU systems were trying to treat too much metal.[5]

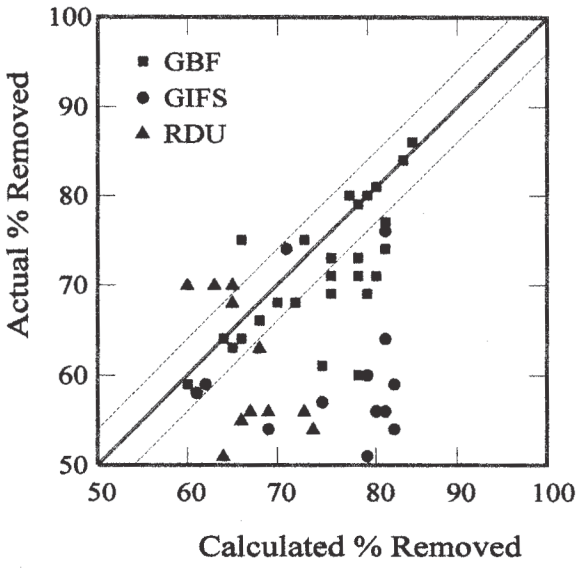

Figure 7. Comparison of Theoretical Model With Production Results

Concluding Remarks

In this paper we have presented a simple and robust model of the degassing process. The equations given herein can be used with

[5] This is particularly true for the RDU. Some of the data for this unit at high flow rates has been excluded, as it would represent an unfair comparison to the other systems, where two stages were employed.

some confidence to model your degassing system, and to help you optimize metal quality and/or reduce production costs.

It is a common practice to add varying amounts of chlorine to the flux gas during the degassing process. Chlorine is often required to remove reactive impurity elements present in the melt. Sodium and sometimes lithium report to the metal from the electrolyte. Both must be removed to very low levels, less than a few ppm, for acceptable product quality. Magnesium, and occasionally other alkali metals, must frequently be removed in the recycling and treatment of secondary alloys.

There is a good deal of confusion in the literature regarding the effect of chlorine additions to the purge gas on the hydrogen removal. Many authors have asserted that chlorine improves the degassing process by the chemical reaction:

$$1/2\ Cl_2 + \underline{H} = HCl\ (v) \qquad (19)$$

This is extremely unlikely, however. Simple thermodynamic calculations can be made from tabulated standard free energies of formation [27]. These show that HCl vapor is much less stable than the aluminum chlorides at temperatures where liquid metal is found.

Botor [15] has shown that chlorine will increase the rate of hydrogen transfer to the bubbles, by as much as a factor of two. This may be an important consideration in some cases, when large bubbles are present. But we have seen above that the purge gas will be close to its thermodynamic equilibrium, and nearly saturated with hydrogen, in any well designed treatment system. When thermodynamic equilibrium applies, the rate of the diffusion-controlled degassing process is so rapid, that it no longer limits the process. Thus, contrary to popular belief, the use of chlorine in the flux gas should have no appreciable benefit as far as hydrogen removal is concerned.

It may also be useful to conclude with a few remarks regarding inclusion removal during gas fluxing of molten aluminum. My past experience in the production of x-ray quality castings has established that gas purging with small bubbles can effectively remove oxide inclusions. A theoretical analysis of the possible inclusion removal mechanisms, and a review of some of the available experimental data is given in [28]. Inclusion removal was also studied in [24, 29-31]. My plant trials also showed that adding small amounts of chlorine to the flux gas significantly improved inclusion removal. The dross produced was also drier.

Removing inclusions, by gas fluxing or filtration, will significantly affect the results obtained when a reduced pressure test (RPT) is employed to measure gas content [32,33]. For this reason, some melters believe it is possible to filter gas out of the metal. Since chlorine assists in inclusion removal during gas purging, and would thereby result in a RPT sample having less porosity, this is probably the reason why small amounts of chlorine in the purge gas has the reputation of removing gas in the metal. But this conclusion is usually erroneous. I have taken RPT and Ransley pin samples before and after a filter. The RPT samples showed a significant difference in porosity level, but the Ransley samples contained the same amount of dissolved hydrogen.

Acknowledgements

The author gratefully acknowledges the Reynolds Metals Company, and the U.S. Department of Energy, whose financial assistance have made this study possible.

List of Symbols

A	Surface area of bubbles in reactor (m^2)
B'	*A constant equal to 3.32 (kg-min/l-sec)*
C	Correction factor for hydrogen solubility
C_e	Exiting concentration of an impurity element (cm^3/100 g, wt%, or ppm)
C_o	Original (entering) concentration of an impurity element (cm^3/100 g, wt%, or ppm)
d	Diameter of bubble (m)
D	Diffusion Coefficient (m^2/sec)
E	Energy of stirring (watts)
e_H^j	First order interaction coefficient (1/wt%)
f_H	Activity coefficient of hydrogen
g	Gravitational constant (m/sec^2)
$\dot{G}$	Flow rate of inert gas (l/min)
$\underline{H}$	Dissolved hydrogen content (cm^3/100 g)
k	Mass transfer coefficient (m/sec)
M	Mass of metal in batch refining (kg)
$\dot{M}$	Mass flow of metal in in-line treatment (kg/min)
P	Pressure of Hydrogen gas (atm)
P_{inert}	Pressure of inert gas (atm)
r_H^j	Second order interaction coefficient ($wt\%^{-2}$)
S	Gas solubility at a hydrogen pressure of one atmosphere (cm^3/100 grams-$atm^{-1/2}$)
t	The degassing time (sec)
T	Thermodynamic temperature (Kelvin)
U	Steady state rise velocity of bubble (m/sec)
$\%j$	Concentration of element j in aluminum (wt%)
β	$\frac{\dot{M}P_{inert}C^2S^2}{100 \cdot \dot{G}}$ (cm^3/100 g)
ρ	Density of molten aluminum (c. 2700 kg/m^3)
σ	surface tension of the metal (J/m^2); also the statistical standard deviation
τ	$2MP_{inert}C^2S^2/\dot{G}B'$ (sec)

References

1. G. K. Sigworth and T. A. Engh: Chemical and Kinetic Factors Related to Hydrogen Removal from Aluminum," Metallurgical Transactions B, 13B (1982), 447-460.
2. R.Y. Lin and M. Hoch: "The Solubility of Hydrogen in Molten Aluminum Alloys," Metallurgical Transactions A, 20A (1989), 1785-1791.
3. P.N. Anyalebechi: "Analysis of the Effects of Alloying Elements on Hydrogen Solubility in Aluminum Alloys," Scr. Met. Mat., 33 (1995) 1209-1216.
4. D.E.J. Talbot and P.N. Anyalebechi: "Solubility of Hydrogen in Liquid Aluminum," Mat. Sci. Tech., 4 (1988), 1-4.
5. A. San-Martin and F.D. Manchester: "The Al-H System," J. Phase Equilibria, 13 (1992), 17-21.
6. W. Eichenauer, K. Hatenbach and A. Pebler: "The Solubility of Hydrogen in Solid and Liquid Aluminum," Z. Metallk., 52 (1961), 682-684.
7. A. Sieverts: "Study of Occlusion and Diffusion of Gases in Metals," Z. Physik. Chem., 60 (1907), 129-201.
8. A. Sieverts and W. Krumbhaar: Berichte Deutsche Chem. Ges., 43 (1910), 893.
9. M. Aheng and X. Zhen: "Hydrogen Probe Equipped with a $SrCeO_3$ Based Proton Conductor," Metallurgical Transactions B, 24B:789-794 (1993).
10. C. Wagner: Thermodynamics of Alloys, (Reading, Massachusetts, Addison-Wesley, 1962), 51.
11. J. Chipman: "Atomic Interactions in Molten Alloy Steels," J. Iron Steel Inst., London, 180 (1955), 97-106.
12. C.H.P. Lupis: "Liquid Metals, Chemistry and Physics," S. Beer, editor (New York, NY, Marcell Dekker, 1972), 1-36.
13. P.N. Anyalebechi: "Analysis and Thermodynamic Prediction of Hydrogen Solution in Solid and Liquid Multicomponent Alloys," Light Metals 1998, 827-842.
14. G.K. Sigworth: "A Scientific Basis for Degassing Aluminum," AFS Transactions, 95 (1987), 73-78.
15. J. Botor: "Kinetics of Hydrogen-degassing of molten aluminum by purge gases," Aluminium, 56 (1980), 519-522.
16. T.A. Engh and G.K. Sigworth: "Molten Aluminum Purification," Light Metals 1982, 983-1001.
17. M. Nilmani, P.K. Thay and C.J. Simensen: "A Comparative Study of Impeller Performance," Light Metals 1992, 939-946.
18. S. T. Johansen *et al.*: "The Bubble Size and Mass Transfer Mechanisms in Rotor Stirred Reactors," Light Metals 1997, 663-666.
19. W.C. Eister and W.R. Krumme: "An Evaluation of a SNIF Unit as an Inclusion Removal and Degassing Device," Light Metals 1991, 1171-1177.
20. J.J.J. Chen and J.C. Zhao: "Bubble Distribution in a Melt Treatment Water Model," Light Metals 1995, 1227-1231.
21. Shinji Nagata: Mixing: Principles and Applications, (New York, Kodanh Ltd. and John Wiley and Sons, 1975).
22. E. Eckert: "Method for Fluxing Molten Metal," U.S. Patents 5,616,167 and 5,630,863.
23. Y. Ohno, D.T. Hampton and A.W. Moores: "The GBF Rotary System for Total Aluminum Filtration," Light Metals 1993, 915-921.
24. E.J. Chin *et al.*: "GIFS—A Novel Approach to the In-Line Treatment of Aluminum," Light Metals 1994, 929-936.
25. G.P. Walker, T.A. Zeliznak and S.R. Sibley: "Practical Degassing with the R.D.U.," Light Metals 1989, 777-782.
26. D.T. Hampton, A. Moores and J.L. Tessamdori: "Review and Operation of the Rapid Degassing Equipment for Molten Aluminum," Light Metals 1991, 1159-1163.
27. D.R. Stull and H. Prophet: JANAF Thermochemical Tables, Second Edition, NSRDS-NBS 37, June, 1971. (There are also a number of data supplements published in the J. Physical and Chemical Reference Data.)
28. L.C.B. Martins and G.K. Sigworth: "Inclusion Removal by Flotation and Stirring," pp. 16-1 to 16-28, Proc. 2nd. Intern. Conf. on Molten Aluminum Processing, Orlando, Fla. Nov. 6.7, 1989, Amer. Foundryman's Soc., Des Plaines, Il., 1989.
29. T. Pedersen: Refining Efficiency on Hydrogen, Alkaline Metals and Inclusions in The Hydro Metal Refining System," Light Metals 1991, 1063-1067.
30. D.E. Groteke: "Influence of SNIF Treatment on Characteristics of Aluminum Foundry Alloys," AFS Transactions, 93 (1985), 953-960.
31. W.C. Eister and W.R. Krumme: "An Evaluation of a SNIF Unit as an Inclusion Removal and Degassing Device, Light Metals 1991, 1171-1177.
32. K.J. Brondyke and P.D. Hess: "Interpretation of Vacuum Test Results for Aluminum Alloys," Trans. TMS-AIME, 230 (1964), 1542-46.
33. E.L. Rooy and E.F. Fischer: "Control of Aluminum Casting Quality by Vacuum Solidification Tests," AFS Transactions, 76 (1963), 237-240.